Substrate Recognition by Gelatinase A: The C-Terminal Domain Facilitates Surface Diffusion

Ivan E. Collier,* Saveez Saffarian,† Barry L. Marmer,* Elliot L. Elson,‡ and Greg Goldberg*‡
*Division of Dermatology and ‡Department of Biochemistry and Molecular Biophysics, Washington University School of Medicine, St. Louis, Missouri 63110; and the †Department of Physics, Washington University College of Arts and Sciences, St. Louis, Missouri 63130 USA

ABSTRACT An investigation of gelatinase A binding to gelatin produced results that are inconsistent with a traditional bimolecular Michaelis-Menten formalism but are effectively accounted for by a power law characteristic of fractal kinetics. The main reason for this inconsistency is that the bulk of the gelatinase A binding depends on its ability to diffuse laterally on the gelatin surface. Most interestingly, we show that the anomalous lateral diffusion and, consequently, the binding to gelatin is greatly facilitated by the C-terminal hemopexin-like domain of the enzyme whereas the specificity of binding resides with the fibronectin-like gelatin-binding domain.

INTRODUCTION

The three-dimensional scaffold of vertebrate extracellular matrix (ECM) consists of highly organized, insoluble assemblies of large protein molecules, including collagens, proteoglycans, fibronectin, laminin, etc., giving tensile strength to the tissue (Kreis and Vale, 1999; Yurchenko et al., 1994). Morphogenesis (Damsky et al., 1997; Werb and Chin, 1998), tissue repair (Chiquet, 1999; Trojanowska et al., 1998), angiogenesis (Friedl and Brocker, 2000; Norrby, 1997), uterine involution, and bone resorption (Karsenty, 1999) are characterized by intensified tissue remodeling that begins with degradation of the existing ECM. Resident cells of tissues can secrete a specialized group of enzymes, matrix metalloproteases (MMPs) (Massova et al., 1998), that can degrade ECM macromolecules such as collagens and proteoglycans (Vu and Werb, 2000). Malignant cells can exploit these same proteases to promote tumor invasion and metastasis (Kleiner and Stetler-Stevenson, 1999; Woodhouse et al., 1997). Gelatinases A (GelA) (Collier et al., 1988) and B (GelB) (Wilhelm et al., 1989) are closely related enzymes of this family that, in addition to their catalytic and hemopexin-like carboxyl-end domains, contain a distinct domain composed of three head-to-tail repeats homologous to the type 2 repeat found in fibronectin (FN). The FN domain confers gelatin substrate binding properties to these proenzymes (Collier et al., 1992). The hemopexin-like, carboxyl-terminal domain (GelA-CTD) plays an important role in membrane activation of the enzyme (Brooks et al., 1996; Butler et al., 1998; Deryugina et al., 2000, 1998; Kinoshita et al., 1998; Kolkenbrock et al., 1997; Quigley and Cheresh, 1996; Strongin et al., 1995) and binding of the inhibitors TIMP and TIMP2 (Goldberg et al., 1989, 1992; Fridman et al., 1992; Olson et al., 1997). Its role in substrate recognition, however, remains unclear (Knauper et al., 1997; Murphy and Knauper, 1997; Wilhelm et al., 1987).

MMP-substrate interactions have been studied applying the Michaelis-Menten formalism based on traditional mass-action kinetics. However, when reactions are restricted to two or fewer dimensional spaces, as can exist in the ECM in vivo, fractal kinetics (Avnir, 1989; Havlin, 1989; Kopelman, 1988) provides a better description of bimolecular reactions. Here we present a serial model for GelA substrate recognition and show the binding to be dependent on anomalous diffusion of the enzyme on the gelatin surface.

MATERIALS AND METHODS

Enzyme purification and labeling

Cells were grown in RPMI 1640 supplemented with 2 mM glutamine and 5% fetal calf serum. GelA proenzyme was purified from conditioned medium of p2aHT7211A cells (Strongin et al., 1993). The truncated mutant of GelA (GelA-Tr) lacking the hemopexin-like carboxyl-end domain was prepared from conditioned medium of p2AHT2a (Frisch et al., 1990) transiently transfected with expression plasmid psg5 bearing an insert coding for GelA Met1-Leu 461. The predicted molecular mass of the GelA-Tr, 48,229 Da, was in good agreement with that determined by SDS/PAGE.

All binding experiments were performed with biosynthetically labeled enzyme to assure the integrity of the protein that might be compromised upon labeling in vitro. For biosynthetic labeling of proteins, cells were transferred into Met-deficient medium containing 50 μCi/ml of *trans*[^{35}S] label (ICN Radiochemicals, Costa Mesa, CA, 1000Ci/mM) 12 h before harvesting the secreted enzyme.

For fluorescence photobleaching recovery (FPR) experiments, purified enzymes were tagged with fluorescent dye Alexa Fluor 488. To prevent interference of the dye with the gelatin-binding site the reaction was performed on the enzyme bound to gelatin as described below. The purified GelA and truncated mutant were labeled with the Alexa Fluor 488 protein labeling kit (Molecular Probes, Eugene, OR), and 100 μg of either protein was adsorbed onto a 100-μl bed volume column of gelatin agarose (Sigma G-5384, Sigma Chemical Co., St. Louis, MO) equilibrated with 25 mM HEPES buffer, pH 7.5, containing 150 mM NaCl and 2 mM $CaCl_2$ at 4°C. A 250-μl volume of Alexa 488 dye (50% of the vial content) dissolved in

Received for publication 30 April 2001 and in final form 19 June 2001.

Address reprint requests to Dr. Greg Goldberg, Washington University School of Medicine, 660 South Euclid Street, St. Louis, MO 63110. Tel.: 314-362-8172; Fax: 314-362-8159; E-mail: goldberg@medicine.wustl.edu.

0006-3495/01/10/2370/08 $2.00

column buffer was added to a dry column and incubated in the dark for 45 min at room temperature with agitation. Columns were washed with the same buffer and eluted with buffer containing 10% dimethylsulfoxide. Proteins were dialyzed into 25 mM HEPES buffer, pH 7.5, containing 0.005% Brij 35. This protocol yielded the fluorescent enzyme labeled with 1 mol of dye per mol of enzyme on average. Both biosynthetically labeled and Alexa Fluor-488-tagged enzymes were stable at room temperature for the duration of the experiments.

Binding measurement and analysis

Enzyme binding was measured at room temperature. Polystyrene Flashplates plates (New England Nuclear, Boston, MA) were used according to manufacturer's instructions to determine binding of ^{35}S biosynthetically labeled enzymes. The wells of the Flashplates plates were coated with 100 μl of gelatin (Biorad, Richmond, CA; 2 μg/ml) in 10 mM Tris-HCl buffer, pH 7.5. Control wells were coated with 100 μl of bovine serum albumin (BSA; 1 mg/ml) in the same buffer. After 1 h, wells were rinsed and incubated overnight at 4°C with 100 μl of 25 mM HEPES buffer, pH 7.5, containing 1 mg/ml BSA, 150 mM NaCl, and 0.005% Brij-35 (BB, binding buffer). All binding measurements were performed in the BB buffer containing 1×10^{-5} M metalloprotease inhibitor SC67787 (BBI buffer). To measure binding in real time, solutions containing radiolabeled ligands in BBI buffer were added simultaneously to the gelatin-coated and control wells, which were counted simultaneously at the indicated times using a Packard TopCount scintillation counter. The specific ligand binding was the difference in cpm of the gelatin- and the BSA-coated wells divided by the molar specific activity of the ligand in units of cpm μmol^{-1}. An arbitrary unit of micromoles per well (μmol well^{-1}) is introduced for convenience to express the surface concentration of ligand bound. Where necessary, it is converted to absolute units using a value of 0.55 ± 0.1 cm^2 for the absorbing area of the well.

For measurements of ligand binding where time was not an independent variable, the plates were incubated for 90 min and the solution containing the ligand removed by blotting the inverted plate before counting as above.

The bimolecular reaction scheme for binding of a ligand in solution to gelatin is:

$$\mathrm{X} + \mathrm{M} \underset{k_\mathrm{d}}{\overset{k_\mathrm{f}}{\leftrightarrow}} \mathrm{MX},$$

where X stands for the ligand, M for gelatin, and MX for their complex. If the ligand solution concentration, $x0$, is constant, then conventional kinetics yields the well known expressions for the amount of complex, mx, formed with respect to time, t:

$$mx = mx_{\mathrm{mx0}} \times \{1 - \exp[-k_\mathrm{a} t]\}, \quad (1.1)$$

where

$$mx_{\mathrm{mx0}} = m0 \times x0 \times k_\mathrm{f} \times (k_\mathrm{d} + x0 \times k_\mathrm{f})^{-1} = b \times m0 \times x0/(1 + b \times x0) \quad (1.2)$$

The equilibrium binding constant is

$$b = k_\mathrm{f}/k_\mathrm{d}. \quad (1.3)$$

The apparent time constant is

$$k_\mathrm{a} = k_\mathrm{f} \times x0 + k_\mathrm{d} = b \times k_\mathrm{d} \times x0 + k_\mathrm{d}. \quad (1.4)$$

If a competing species is present with concentration $i0$, Eq. 1.2 becomes

$$mx_{\mathrm{mx0}} = b \times m0 \times x0/(1 + bi \times i0 + b \times x0), \quad (1.5)$$

where bi is the equilibrium binding constant of the competing ligand.

The serial reaction scheme for binding of a ligand to gelatin is:

$$\begin{array}{ccc} & \overset{k_\mathrm{snf}}{\underset{k_\mathrm{snd}}{\rightleftarrows}} \mathrm{S_nX + I + M} \xrightarrow{k_\mathrm{snm}} \mathrm{S_n + I + MX} & \\ \mathrm{Sn + X + I + M} & & n = 1, 2, 3 \\ & \overset{k_\mathrm{snf}}{\underset{k_\mathrm{snd}}{\rightleftarrows}} \mathrm{S_nI + X + M} \xrightarrow{ki_\mathrm{snm}} \mathrm{S_n + X + MI}, & \end{array}$$

where X stands for the ligand and I for its competitor. S_1 through S_3 stand for gelatin sites associated with the first step in the binding reaction, and S_1X through S_3X or S_1I through S_3I for their complexes with the ligand or its competitor. M represents gelatin sites associated with the second step of the binding reaction, and MX and MI represent their complexes with the ligand or its competitor. In the first step of the binding reaction, a ligand or competitor in solution binds at one of the S sites. In the second reaction, a ligand or competitor bound to one of the S sites translocates to one of the M sites that are inaccessible directly from solution. The rate constants for competitor binding to the S sites are identical to those of the ligand itself, whereas the rate constants for translocation of the competitor to the M sites may be different from that of the ligand itself.

If the binding to precursor S sites by ligand or competitor is in equilibrium, then the amount of ligand-S site complex of each kind is:

$$s_\mathrm{n}x = s_\mathrm{n}0 \times b_\mathrm{n} \times x0/(1 + b_\mathrm{n} \times i0 + b_\mathrm{n} \times x0) \quad (2.0a)$$

and

$$s_\mathrm{n}i = s_\mathrm{n}0 \times b_\mathrm{n} \times i0/(1 + b_\mathrm{n} \times i0 + b_\mathrm{n} \times x0); \quad n = 1, 2, 3, \quad (2.0b)$$

where $b_\mathrm{n} = k_{\mathrm{snf}}/k_{\mathrm{snd}}$, and the equilibrium binding constant of the ligand, b_n, and that of competitor species are identical according to the model assumptions (see above). The $s_\mathrm{n}0$ are the total density of S sites of the of the nth ($n = 1, 2, 3$) class, and $x0$ and $i0$ are the constant solution concentrations of the ligand and competitor species, respectively. Fractal-like kinetics (Kopelman, 1988) yields the following rate equation for the irreversible formation of the MX or MI complexes from the S_NX or S_NI complexes:

$$d(mx)/dt = \sum_{\mathrm{n}=1}^{3} k_{\mathrm{snm}} \times t^{-\mathrm{h}} \times s_\mathrm{n}x \times (m0 - mx - mi) \quad (2.0c)$$

$$d(mi)/dt = \sum_{\mathrm{n}=1}^{3} ki_{\mathrm{snm}} \times t^{-\mathrm{h}} \times s_\mathrm{n}i \times (m0 - mx - mi). \quad (2.0d)$$

Equations 2.0a and 2.0b are integrated give the expression:

$$mx = \frac{m0\ \mathrm{sum}x0 - \left[\dfrac{e^{(-\mathrm{sum}i0 - \mathrm{sum}x0)\tau}\, m0\ \mathrm{sum}i0\ \mathrm{sum}x0}{\mathrm{sum}i0 + \mathrm{sum}x0}\right] - \left[\dfrac{e^{(-\mathrm{sum}i0 - \mathrm{sum}x0)\tau}\, m0\ \mathrm{sum}x0^2}{\mathrm{sum}i0 + \mathrm{sum}x0}\right]}{\mathrm{sum}i0 + \mathrm{sum}x0} \quad (2.1)$$

for mx as a function $x0$, $i0$, and t, where:

$$\mathrm{sum}x0 = \sum_{n=1}^{3} k_{\mathrm{snm}} \times s_{\mathrm{n}}x, \tag{2.2a}$$

$$\mathrm{sum}i0 = \sum_{n=1}^{3} ki_{\mathrm{snm}} \times s_{\mathrm{n}}i, \tag{2.2b}$$

and

$$\tau = t^{(1-\mathrm{h})}/(1-h). \tag{2.3}$$

In the absence of inhibitor, the M site binding (Eq 2.1) is given by:

$$mx = m0 \times (1 - e^{-\mathrm{sum}x0\tau}). \tag{2.4}$$

When

$$t^{(1-\mathrm{h})} \times m0 \times \mathrm{sum}x0 \times (1-h)^{-1} \le 0.15,$$

then

$$mx \approx t^{(1-\mathrm{h})} \times m0 \times \mathrm{sum}x0 \times (1-h)^{-1}. \tag{2.5}$$

FPR measurement and analysis

FPR measurements were performed as described (Petersen and Elson, 1986) at room temperature. One side of 1.2-cm-diameter glass coverslips was covered with 100 μl of gelatin solution (2 μg/ml in 10 mM Tris-HCl buffer, pH 7.5) and incubated overnight in a closed humidified chamber. The gelatin-coated coverslips were rinsed exhaustively with BBI before 50 μl of either fluorescently labeled (FL) GelA (1 μM in BBI) or GelA-Tr (3 μM in BBI) were applied. The samples were incubated for 1 h in the dark and the excess of ligand removed by washing the coverslips with BBI buffer. The coated side of the coverslip was placed on top of a glass slide with 2 μl of BBI buffer, and the edge of the coverslip was sealed before FPR measurements. For delayed measurements, the coated side of the coverslip was floated on top of a 50-μl drop of BBI buffer and incubated for 1 h before being prepared for FPR measurement as above.

The analysis of FPR data has been described (Axelrod et al., 1976). The following modifications accommodate continuous monitor beam photobleaching. Let K be the bleach parameter; T, time of bleach; l, photochemical quantum yield; D, diffusion coefficient; $c0$, initial uniform concentration of diffusing fluorophore; w, the beam radius at exp(−2) of its central intensity; and $I_{0\mathrm{B}}$ and $I_{0\mathrm{M}}$, the central maxima of bleaching and monitor beams. The partial differential equation,

$$\partial c(r,t)/\partial t = D\nabla^2 c(r,t) - c(r,t)\lambda I_{0\mathrm{M}}\exp[-2(r/w)^2], \tag{3.0a}$$

and the initial condition,

$$c(r,0) = c0, \tag{3.0b}$$

describe the self-diffusion of an initially uniform distribution of mobile fluorophores in the presence of continuous monitor beam photobleaching. Equation 3a and the initial condition,

$$c(r,0) = c0\,\exp\{-\lambda I_{0\mathrm{B}} T \exp[-2(r/w)^2]\},$$
$$K = \lambda I_{0\mathrm{B}} T, \tag{3.0c}$$

describe the self-diffusion of a non-uniform distribution of bleached mobile fluorophores in the presence of continuous monitor beam photobleaching. Eq. 3.0a together with either 3.0b or 3.0c is integrated numerically (Wolfram, 1999), subject to the forced boundary conditions,

$$\partial c(r\mathrm{B},t)/\partial r = 0,\ r\mathrm{B} = 10w$$
$$\partial c(r_0,t)/\partial r = 0, \quad r_0 = w(8000)^{-1}$$

to yield, respectively, the time-dependent concentration profile of fluorophores before, $c_{\mathrm{P}}(r,t)$, or after, $c_{\mathrm{R}}(r,t)$, photobleaching. The fluorescence in arbitrary units, $a(t)$, at time t is obtained from:

$$a(t) = \phi\int c_{\mathrm{P}}(r,t)\exp[-2(r/w)^2]\,2\pi r dr + (1-\phi)F_{-}(t);$$
$$t < \text{ time of bleach}$$
$$a(t) = \phi\int c_{\mathrm{R}}(r,t)\exp[-2(r/w)^2\,2\pi r dr + (1-\phi)F_{+}(t);$$
$$t > \text{time of bleach}, \tag{3.1}$$

where ϕ is the fraction of fluorophores that are mobile and

$$F_{-}(t) = c0 \times w^2 \times p \times \{1 - exp(-\lambda I_{0\mathrm{M}} t)\} \times (2lt)^{-1}$$
$$F_{+}(t) = c0 \times w^2 \times p \times \{1 - \exp[-\lambda I_{0\mathrm{M}}(t+TR)]\}$$
$$\times \{2\lambda(t+TR)\}^{-1}; \quad R = I_{0\mathrm{B}}/I_{0\mathrm{M}}.$$

The relative fluorescence is defined as

$$r(t) = a(t)/a(-), \tag{3.2}$$

where $a(-)$ is the fluorescence immediately before the bleach.

Experimental values for D and ϕ were calculated iteratively from fluorescence recovery data normalized in accordance with Eq. 3.2. The parameter w has been previously determined for each objective lens as described (Axelrod et al., 1976). Given estimated values of D and ϕ, $\lambda I_{0\mathrm{M}}$ and R were determined from the prebleach and immediate postbleach portions of the recovery curves, respectively. Improved values of D and ϕ were then obtained by incrementally varying their value until a minimum in the χ^2 statistic for the entire recovery curve was obtained. These procedures were implemented using the Mathematica (Wolfram Research, Champaign, IL) system. To fit anomalous diffusion recovery curves to the data, the recovery time t at each data point was replaced with $t^{1/\alpha}$ Then all parameters were determined as described above.

RESULTS AND DISCUSSION

Interaction of gelatinase A with gelatin is described by a sequential binding model with fractal-like kinetics

We have shown that the FN domain enables binding of GelA proenzyme to gelatin (Collier et al., 1992). Recombinant GelA-CTD does not bind gelatin (Collier and Goldberg, unpublished data) and, accordingly, does not compete the enzyme binding (see Fig. 2, open triangles) providing further evidence that binding specificity resides in the FN domain. The apparent equilibrium binding of ^{35}S-labeled GelA can be described (Fig. 1 *B*) by a single binding

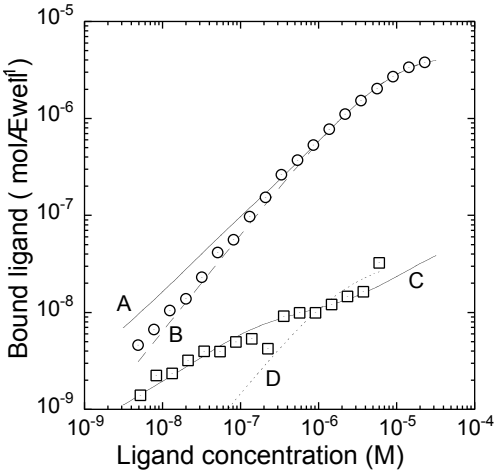

FIGURE 1 The concentration dependence of GelA (○) and GelA-Tr (□) binding. A 50-μl volume of either ^{35}S-GelA or ^{35}S-GelA-Tr in BBI buffer was diluted to reach final concentrations as indicated and added to Flashplates (Du Pont NEN) that were incubated for 90 min and counted. The amount of GelA- or GelA-Tr-specific binding to gelatin is plotted on double logarithmic axes versus the concentration of the ligand. (*A*) Fit of Eq 2.4 (t = 90min) to the wild-type binding data. (B) Unweighted two-parameter nonlinear least-squares fit of Eq. 1.2 to the wild-type binding data. (*C*) Fit of the sum of Eq 2.0a (binding to S sites) and 2.4 (binding to M sites) to the mutant (GelA-Tr) binding data subject to the constraint that S and M sites contribute equally to the total. (*D*) Unweighted two-parameter nonlinear least-squares fit of Eq. 1.2 to the mutant (GelA-Tr) binding data.

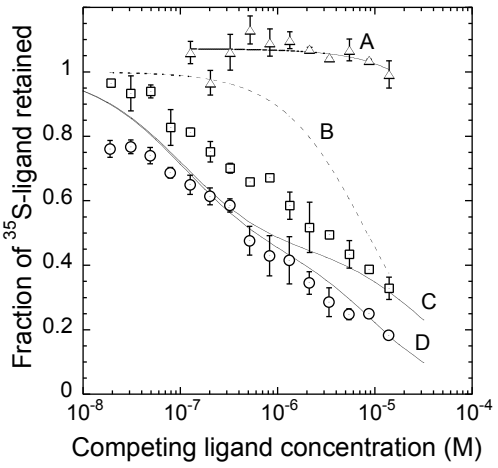

FIGURE 2 Competition of gelatin binding by in vivo labeled ^{35}S-GelA with unlabeled GelA (○), GelA-Tr (□), and GelA-CTD (△). A 50-μl volume of ^{35}S-GelA (0.015 μM and 3.34×10^9 cpm/L) containing unlabeled GelA, GelA-Tr, or GelA-CTD at the indicated molarity was added to Flashplates (Du Pont NEN) that were incubated for 90 min and counted. The amount of GelA-specific binding to gelatin expressed as a fraction of the binding in the absence of competing ligand is plotted versus the molarity of the competing ligand. The error bars along the ordinate are the differences in the duplicate samples. (*A*) Linear regression on the 35 S GelA competition by the recombinant GelA-CTD data. (*B*) Predicted competition of GelA for a one-step process, Eq. 1.5, by a competitor with both having an identical equilibrium binding constant of 1.2×10^5 M^{-1}. (*C* and *D*) Competition of GelA by GelA-Tr or GelA itself, respectively, predicted by the two-step binding model, Eq. 2.1.

isotherm, Eq. 1.2 (see Materials and Methods), with an apparent binding constant of 1.2×10^5 M^{-1} and site density of 5.2×10^{-6} μmol well^{-1}. Surprisingly, the truncated mutant of GelA (GelA-Tr) lacking the GelA-CTD has a poor gelatin-binding capacity (Fig. 1), and a single isotherm (Fig. 1 *D*) fits the data poorly. To explain these results we first considered a model with heterogeneous binding sites. A minimum of three independent binding sites having densities of 10^{-8}, 1.9×10^{-7}, and 5.2×10^{-6} μmol well^{-1} and corresponding equilibrium constants of 2.5×10^7 M^{-1}, 2.0×10^3 M^{-1}, and 5.4×10^2 M^{-1} were required to approximate the GelA-Tr binding data (Fig. 1). A change in affinity of the three sites to 1.9×10^8, 7.5×10^5, and 1.2×10^5 M^{-1} produced an adequate description of the wild-type enzyme binding (Fig. 1) and competition experiments (Fig. 2). We found, however, that the GelA-Tr is able to compete the binding of GelA much beyond what would be expected from its poor binding ability (Fig. 2). Thus, conventional binding models with either single or heterogeneous binding sites failed to account for the binding and the competition behavior of the GelA-Tr. To further understand the mechanism of GelA and GelA-Tr binding to gelatin we examined the kinetics of dissociation (Fig. 3) and association (Fig. 4) for both enzyme forms.

GelA desorption (Fig. 3) was independent of initial surface concentration, which was varied from 5×10^{-8} to 6×10^{-7} μmol well^{-1}. A fit of a single-exponential decay to the dissociation data (Fig. 3 *C*) yielded $k_d = 7.5 \pm 1.7 \times 10^{-4}$ min^{-1}, demonstrating that binding is practically irreversible (Fig. 3 *A*) with a half-life of 15 h. GelA-Tr dissociation was also independent of initial surface concentration, which varied from 1.4×10^{-9} to 3×10^{-8} μmol well^{-1}, but exhibited a fast mode of decay in addition to a slow mode identical to that of wild type (Fig. 3 *B*). GelA association time courses (Fig. 4) fitted to an exponential association curve, Eqs. 1.0–1.5, yielded apparent time constants, k_a, which were independent of ligand concentration with a mean value of 0.081 ± 0.014 min^{-1}. This result together with the equilibrium binding constant of the dominant binding component (1.0×10^5 M^{-1}) and Eq. 1.4, suggest that GelA binding should be significantly reversible with a k_d of 0.08 min^{-1}. This value is two orders of magnitude greater than the k_d determined above, indicating that conventional kinetic mechanisms of binding and dissociation are inadequate to describe this system.

A power-law time dependence characteristic of fractal kinetics (Avnir, 1989; Dewey, 1997; Havlin, 1989; Kopelman, 1988) produces a closer fit to association data (Fig. 4) and suggests the way to resolve the contradiction. Fractal kinetics implies that the binding reaction slows and appears complete because it is self-limiting rather than because it is approaching equilibrium. Thus, rate constants are replaced

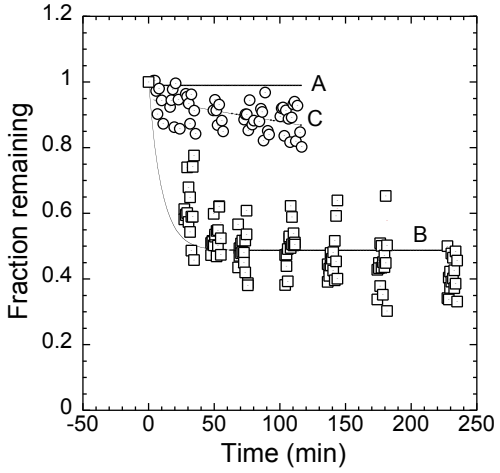

FIGURE 3 Gelatin dissociation time courses of labeled ^{35}S-GelA (○) and GelA-Tr (□). Association reactions for GelA and GelA-Tr were performed as described in Fig. 4 for enzyme concentrations ranging from 0.06 μM to 1.1 μM and 0.005 μM to 6 μM, respectively. After 110 min of association reaction, the unadsorbed enzymes were replaced with buffer and the amount of radioactivity associated with the wells was determined at the indicated times. The GelA or GelA-Tr dissociation data were normalized to the initial surface concentration and combined. (*A*) GelA dissociation predicted by the two-step binding model where 99% (M sites) of the binding is irreversible and 1% (S sites) decays exponentially with a time constant of 0.1 min^{-1}. (*B*) A similar dissociation curve for GelA-Tr where the distribution between the S and M sites is 50/50. (*C*) Fit of a single-exponential decay to the GelA dissociation data having a $k_d = 7.5 \pm 1.7 \times 10^{-4}$ min^{-1}.

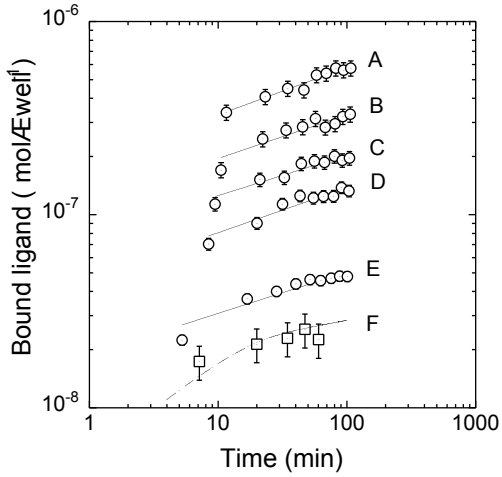

FIGURE 4 The association time course of GelA (○) and GelA-Tr binding (□). A 50-μl volume of either ^{35}S-GelA or ^{35}S-GelA-Tr in BBI buffer was diluted to reach final concentrations as indicated and added simultaneously to the gelatin (200 ng/well) or BSA-coated wells of Flashplates (Du Pont NEN). The radioactivity associated with the wells was monitored in real time and the amount of specific binding was plotted versus the time after the addition of the ligand on double logarithmic axes. The error bars were calculated from the signal-to-noise ratio of the control (BSA) and gelatin wells. (*A–E*, ——) Two-parameter nonlinear least-squares fits of the GelA association data at each concentration (1.1, 0.65, 0.38, 0.22, and 0.06 μM, respectively) to Eq. 2.5. (*F*) Gelatin association time course predicted for the mutant (GelA-Tr) by the sequential model of binding It is the sum of rapid exponential association to the S sites (50%) and a fractal-like association to the M sites (50%), Eq. 2.4 with $h = 0.75 \pm 0.015$.

with time-dependent rate coefficients, kt^{-h} where k is a constant and h is the fractal exponent ($0 \leq h \leq 1$), characteristic of the particular reaction system. Fractal kinetics applied to a two-step sequential binding mechanism explains the binding behavior of GelA and GelA-Tr. In this model (see Materials and Methods), adsorption of both GelA and GelA-Tr from solution occurs at heterogeneous (minimum of three) sites, S, constituting 1% or less of total binding. Subsequently, the S-site-bound GelA translocates to a second tier of binding sites, M, comprising the remainder of gelatin binding. The GelA-Tr is deficient in translocation and thus cannot occupy the M sites to the extent that GelA can. Due to the bottleneck effect created by the limited number of accessible S sites, GelA-Tr effectively competes GelA binding despite occupying few M sites. The application of fractal kinetics to the translocation step of this binding model produced a quantitative description of binding data with a fractal constant $h = 0.75$ in Eqs. 2.0–2.4. This value of h allows fitting Eqs. 2.4 and 2.1 to the GelA binding concentration dependence (Fig. 1 *A*) and the competition data (Fig. 2 *D*). The irreversible S-to-M translocation approximates the slow GelA dissociation (Fig. 3 *A*), and the power-law Eq. 2.5 accounts for the time course binding data (Fig. 4, *A–E*).

A reduction of the translocation rate constant in Eq. 2.1 is sufficient to describe the binding behavior of GelA-Tr. Because little GelA-Tr translocates from S to M sites during the time period of the measurement, the mutant binding (Fig. 1 *C*) is the sum of binding to S sites, Eq. 2.0a, and M sites, Eq. 2.4, each accounting for half of the total. In consequence, the time course of GelA-Tr dissociation can be represented as the sum of a single exponential describing the reversible S-site desorption and a constant representing irreversible M-site binding (Fig. 3 *B*). Furthermore, the exponential decay has a k_d on order of 0.1 min^{-1}. This value agrees with the mutant association data (Fig. 1 *C*; Fig. 4 *F*) when approximated as the sum of rapid S-site binding and slower M-site binding.

The above model assumes prior equilibrium binding at the reversible S sites for both GelA and GelA-Tr, making translocation the rate-limiting step. Hence, the overall fractal nature of GelA binding can be attributed to the translocation reaction. We hypothesize that the S-to-M translocation involves diffusion of the enzyme on the gelatin surface.

The C-terminal domain of gelatinase A facilitates substrate recognition by enabling lateral diffusion on the gelatin surface

We used fluorescence photobleaching recovery (see Materials and Methods) to test the ability of fluorescently labeled

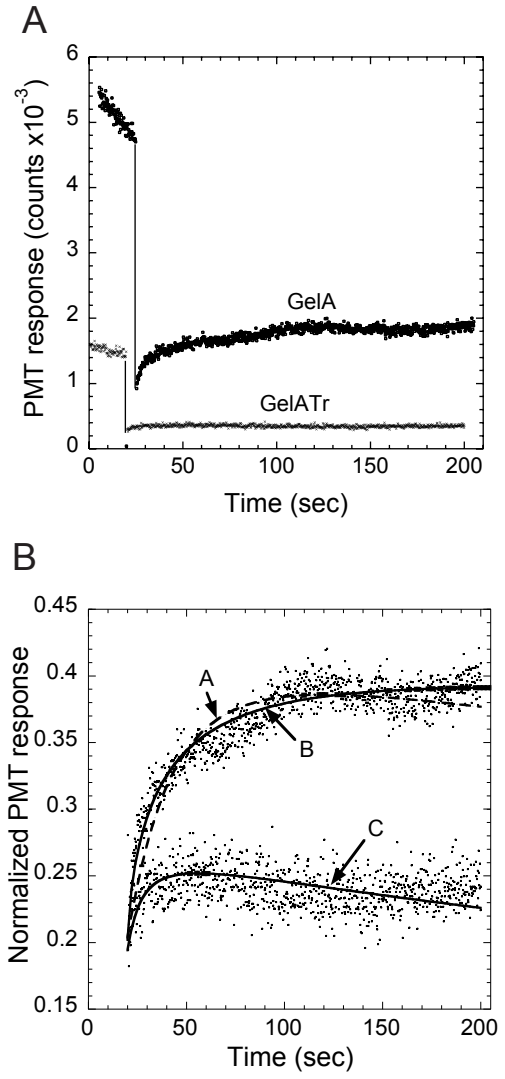

FIGURE 5 Fluorescence photobleaching recovery from gelatin-adsorbed fluorescently labeled GelA and GelA-Tr. Fluorescently labeled enzymes GelA (1 μM) or GelA-Tr (3 μM) were prepared and applied to glass coverslips. Fluorescence was excited with the attenuated beam (10^{-4} attenuation ratio) from an argon-ion laser (488 nm) and was observed with a 40× microscope objective. Fluorescence was monitored for 20 s before and 180 s after a 200-ms bleaching pulse (0.7 attenuation ratio). (*a*) The complete record of an FPR experiment expressed as PMT response in counts is plotted versus the time after the start of the experiment. The record for GelA is displaced forward by 5 s for clarity. (*b*) Normalized fluorescence recovery, Eq 3.2. (*A*) Fit of Eq 3.2 to the wild-type recovery data; (*B*) Fit of Eq. 3.2 to the wild-type recovery data corrected for anomalous diffusion.

GelA and GelA-Tr to diffuse laterally on a gelatin substrate. The isolated recovery phase of the entire FPR experiment (Fig. 5 *a*) is seen in Fig. 5 *b* where the signal has been normalized to the value of fluorescence just before photobleaching. The results clearly demonstrate that the recovery of the GelA-Tr fluorescence is significantly reduced compared with the wild-type enzyme (Fig. 5). Recovery curve analysis (Axelrod et al., 1976) was modified (see Materials and Methods) to account for significant monitor beam photobleaching apparent in the prebleach portion of the experiment (Fig. 5 *a*). Curve *A* (Fig. 5 *b*) is the predicted diffusion-dependent recovery curve for a diffusion coefficient of 0.4×10^{-9} cm^2 s^{-1} and a mobile fraction of 0.42 resulting from a least-squares fit of Eq. 3.2 to the data. Such fitted curves consistently underestimated the recovery in the first 20–25 s after photobleaching in all data sets. Likewise, curves fit to the first 30 s of recovery using Eq. 3.2 consistently underestimated the total recovery at 100–200 s, suggesting that the recovery data had a long tail (results not shown). Webb and co-workers (Feder et al., 1996) have shown that long time tails in FPR may arise from anomalous diffusion (Bouchaud and Georges, 1990) when recovery becomes a function of t^{α} (<1) rather than t as for Brownian diffusion.

To test whether the GelA FPR is better described by an anomalous diffusion, the data from four independent FPR measurements were fit (Fig. 5 *b*, curve *B*) using Eq. 3.2, modified to account for anomalous diffusion and compared with the normal diffusion, Eq. 3.2, using the χ^2 statistic. The observed differences favored the anomalous diffusion with a 95% confidence level by Student's *t*-test (compare Fig. 5, curve *A* with curve *B*). The average anomalous transport coefficient was $2.1 \pm 0.5 \times 10^{-9}$ cm^2 s^{-1} with an average mobile fraction of 0.33 ± 0.03 when $\alpha = 0.66$. A lower signal-to-noise ratio combined with significantly reduced recovery in the GelA-Tr FPR experiments did not permit a distinction between normal and anomalous diffusion. The GelA-Tr recovery curves (Fig. 5 *b*, curve *C*) based on normal diffusion were fit to the data with no obvious pattern of deviation as was observed for the GelA. An average diffusion coefficient of $2.1 \pm 1.0 \times 10^{-9}$ cm^2 s^{-1} and mobile fraction of 0.12 ± 0.02 were obtained.

Data analysis using either anomalous (GelA) or regular (GelA-Tr) diffusion showed that only a fraction of the enzyme is mobile at any given time. The size of the mobile fraction decreased with increasing incubation time. If samples were bound to gelatin (see Materials and Methods) for an hour before analysis, the mobile fraction fell to ~0.10 in the case of GelA and no detectable recovery was observed for GelA-Tr. Thus, it appears that after a period of mobility on the gelatin layer the ligand becomes fixed, perhaps reflecting the essentially irreversible nature of binding to M sites.

Finally, to confirm that the signal recovery in GelA FPR experiments is due to a diffusion process, we have compared the data collected with 16× and 40× microscope objectives (Feder et al., 1996). Taking account of the 2.5-fold difference in the size of the illuminated spot (*w* in Eqs. 3), we obtained nearly equal values of the diffusion coefficient ($3.2 \pm 0.3 \times 10^{-9}$ cm^2 s^{-1} and $2.1 \pm 0.5 \times 10^{-9}$ cm^2 s^{-1}), demonstrating that the kinetic process responsible for fluorescence recovery had the spatial characteristics of diffusion of the enzyme on gelatin substrate. Hence, results of

FPR experiments confirm the hypothesis that GelA is capable of an anomalous lateral diffusion on gelatin and that the C-terminal domain facilitates this process. Moreover, the fractal-like nature of the gelatin-binding kinetics could be a direct consequence of the fractal-like anomalous diffusion process.

It is important to note that our results do not necessarily imply that sets of distinct S and M binding sites occur on the ECM substrate in vivo.

The existence of such distinction between the S and M sites may due entirely to properties of the glass-adsorbed gelatin layer. Gelatin, a polyampholyte with an isoelectric pH of 4.9 adsorbs to the glass surface with a relatively flat conformation at low pH. As the pH increases, the attractive interaction between glass and gelatin decreases and the gelatin extends away from the surface causing the layer to swell (Braithwaite et al., 1999). Among other factors the swelling might contribute to a restriction of accessibility of some binding sites. Thus, the S sites are defined as a small subset of binding sites on glass-adsorbed gelatin to which the binding of the truncated mutant is restricted. Moreover, the competition experiments show that the S sites impose a bottleneck effect on the gelatin binding of GelA in this experimental system.

The mechanism of GelA diffusion on its substrate is not clear. The FN-like domain is the prime determinant of the enzyme-gelatin interaction. Lateral diffusion requires a transient interruption of the interaction between gelatin and the FN-like domain. The role of the GelA-CTD could be to promote such a transient effect by interacting directly with the FN-like domain. Supporting this hypothesis are observations that the GelA-CTD can interact with GelA-Tr in solution (Collier and Goldberg, unpublished results) and more specifically with the third repeat of the FN-like domain as revealed by the crystal structure of GelA (Morgunova et al., 1999). In addition, although the recombinant GelA-CTD does not bind to gelatin appreciably, our data do not exclude the possibility of their weak interaction, thus aiding the displacement of the enzyme to nearby binding sites in a stepwise fashion. The repetitive structure of the collagens and gelatin may serve as an ideal substrate for such a process.

What are the implications of these results to the processes of tissue remodeling catalyzed by metalloproteases? Lateral surface diffusion could be a widespread mechanism in the metabolism of ECM where small molecules secreted by resident cells are required to interact at specific sites within large protein assemblies. This circumstance provides an ideal environment in which diffusion at reduced dimensionality produces association rates beyond those that can be supported by simple diffusion in three dimensions. Thus, the rules of fractal kinetics and surface diffusion may provide a more appropriate view on these interactions compared with the rules of solution biochemistry.

We thank Drs. Henning Birkedal-Hansen of National Institutes of Health and Kenneth M Pryse and Arthur Eisen of Washington University School of Medicine for critical reading of the manuscript. We thank Dr. Dan Getman and the Monsanto Company for generously providing us with the metalloprotease inhibitor SC67787.

This work was supported by the grants R01 AR40618 and R01 AR39472 from the National Institute of Arthritis and Musculoskeletal and Skin Diseases (NIAMS, National Institutes of Health) and R01 GM38838 from the National Institute of General Medical Sciences (NIGMS, National Institutes of Health).

REFERENCES

Avnir, D. 1989. Molecular Diffusion and Reactions. *In* The Fractal Approach to Heterogeneous Chemistry. D. Avnir, editor. John Wiley and Sons, New York.

Axelrod, D., D. E. Koppel, J. Schlessinger, E. Elson, and W. W. Webb. 1976. Mobility measurement by analysis of fluorescence photobleaching recovery kinetics. *Biophys. J.* 16:1055–1069.

Bouchaud, J-P., and A. Georges. 1990. Anomalous diffusion in disordered media: statistical mechanisms, models and physical applications. *Phys. Rep.* 195:127–293.

Braithwaite, G. J., P. F. Luckham, and A. M. Howe. 1999. Study of a solvated adsorbed gelatin layer using a modified force microscope. *J. Colloid Interface Sci.* 213:525–545.

Brooks, P. C., S. Stromblad, L. C. Sanders, T. L. von Schalscha, R. T. Aimes, W. G. Stetler-Stevenson, J. P. Quigley, and D. A. Cheresh. 1996. Localization of matrix metalloproteinase MMP-2 to the surface of invasive cells by interaction with integrin alpha v beta 3. *Cell.* 85: 683–693.

Butler, G. S., M. J. Butler, S. J. Atkinson, H. Will, T. Tamura, S. S. van Westrum, T. Crabbe, J. Clements, M. P. d'Ortho, and G. Murphy. 1998. The TIMP2 membrane type 1 metalloproteinase "receptor" regulates the concentration and efficient activation of progelatinase A: a kinetic study. *J. Biol. Chem.* 273:871–880.

Chiquet, M. 1999. Regulation of extracellular matrix gene expression by mechanical stress. *Matrix Biol.* 18:417–426.

Collier, I. E., P. A. Krasnov, A. Y. Strongin, H. Birkedal-Hansen, and G. I. Goldberg. 1992. Alanine scanning mutagenesis and functional analysis of the fibronectin-like collagen-binding domain from human 92-kDa type IV collagenase. *J. Biol. Chem.* 267:6776–6781.

Collier, I. E., S. M. Wilhelm, A. Z. Eisen, B. L. Marmer, G. A. Grant, J. L. Seltzer, A. Kronberger, C. S. He, E. A. Bauer, and G. I. Goldberg. 1988. H-ras oncogene-transformed human bronchial epithelial cells (TBE-1) secrete a single metalloprotease capable of degrading basement membrane collagen. *J. Biol. Chem.* 263:6579–6587.

Damsky, C. H., A. Moursi, Y. Zhou, S. J. Fisher, and R. K. Globus. 1997. The solid state environment orchestrates embryonic development and tissue remodeling. *Kidney Int.* 51:1427–1433.

Deryugina, E. I., M. A. Bourdon, K. Jungwirth, J. W. Smith, and A. Y. Strongin. 2000. Functional activation of integrin alpha v beta 3 in tumor cells expressing membrane-type 1 matrix metalloproteinase. *Int. J. Cancer.* 86:15–23.

Deryugina, E. I., M. A. Bourdon, R. A. Reisfeld, and A. Strongin. 1998. Remodeling of collagen matrix by human tumor cells requires activation and cell surface association of matrix metalloproteinase-2. *Cancer Res.* 58:3743–3750.

Dewey, T. G. 1997. Fractals in Molecular Biophysics. Oxford University Press, New York.

Feder, T. J., I. Brust-Mascher, J. P. Slattery, B. Baird, and W. W. Webb. 1996. Constrained diffusion or immobile fraction on cell surfaces: a new interpretation. *Biophys. J.* 70:2767–2773.

Fridman, R., T. R. Fuerst, R. E. Bird, M. Hoyhtya, M. Oelkuct, S. Kraus, D. Komarek, L. A. Liotta, M. L. Berman, and W. G. Stetler-Stevenson. 1992. Domain structure of human 72-kDa gelatinase/type IV collagenase: characterization of proteolytic activity and identification of

the tissue inhibitor of metalloproteinase-2 (TIMP-2) binding regions. *J. Biol. Chem.* 267:15398–15405.

Friedl, P., and E. B. Brocker. 2000. The biology of cell locomotion within three-dimensional extracellular matrix. *Cell. Mol. Life Sci.* 57:41–64.

Frisch, S. M., R. Reich, I. E. Collier, L. T. Genrich, G. Martin, and G. I. Goldberg. 1990. Adenovirus E1A represses protease gene expression and inhibits metastasis of human tumor cells. *Oncogene.* 5:75–83.

Goldberg, G. I., B. L. Marmer, G. A. Grant, A. Z. Eisen, S. M. Wilhelm, and C. He. 1989. Human 72-kDa type IV collagenase forms a complex with a novel tissue inhibitor of metalloproteases, TIMP-2. *Proc. Natl. Acad. Sci. U.S.A.* 86:8207–8211.

Goldberg, G. I., A. Strongin, I. E. Collier, L. T. Genrich, and B. L. Marmer. 1992. Interaction of 92-kDa type IV collagenase with the tissue inhibitor of metalloproteinases prevents dimerization, complex formation with interstitial collagenase, and activation of the proenzyme with stromelysin. *J. Biol. Chem.* 267:4583–4591.

Havlin, S. 1989. Molecular Diffusion and Reactions. *In* The Fractal Approach to Heterogeneous Chemistry. D. Avnir, editor. John Wiley and Sons, New York.

Karsenty, G. 1999. The genetic transformation of bone biology. *Genes Dev.* 13:3037–3051.

Kinoshita, T., H. Sato, A. Okada, E. Ohuchi, K. Imai, Y. Okada, and M. Seiki. 1998. TIMP-2 promotes activation of progelatinase A by membrane-type 1 matrix metalloproteinase immobilized on agarose beads. *J. Biol. Chem.* 273:16098–16103.

Kleiner, D. E., and W. G. Stetler-Stevenson. 1999. Matrix metalloproteinases and metastasis. *Cancer Chemother. Pharmacol.* 43:S42–S51.

Knauper, V., S. Cowell, B. Smith, C. Lopez-Otin, M. O'Shea, H. Morris, L. Zardi, and G. Murphy. 1997. The role of the C-terminal domain of human collagenase-3 (MMP-13) in the activation of procollagenase-3, substrate specificity, and tissue inhibitor of metalloproteinase interaction. *J. Biol. Chem.* 272:7608–7616.

Kolkenbrock, H., A. Hecker-Kia, D. Orgel, N. Ulbrich, and H. Will. 1997. Activation of progelatinase A and progelatinase A/TIMP-2 complex by membrane type 2-matrix metalloproteinase. *Biol. Chem.* 378:71–76.

Kopelman, R. 1988. Fractal Reaction Kinetics. *Science.* 241:1620–1626.

Kreis, T., and R. Vale, editors. 1999. Guidebook to the Extracellular Matrix, Anchor and Adhesion Proteins, 2nd ed. Oxford University Press, New York.

Massova, I., L. P. Kotra, R. Fridman, and S. Mobashery. 1998. Matrix metalloproteinases: structures, evolution, and diversification. *FASEB J.* 12:1075–1095.

Morgunova, E., A. Tuuttila, U. Bergmann, M. Isupov, Y. Lindqvist, G. Schneider, and K. Tryggvason. 1999. Structure of human pro-matrix metalloproteinase-2: activation mechanism revealed. *Science.* 284: 1667–1670.

Murphy, G., and V. Knauper. 1997. Relating matrix metalloproteinase structure to function: why the "hemopexin" domain? *Matrix Biol.* 15: 511–518.

Norrby, K. 1997. Angiogenesis: new aspects relating to its initiation and control. *APMIS.* 105:417–437.

Olson, M. W., D. C. Gervasi, S. Mobashery, and R. Fridman. 1997. Kinetic analysis of the binding of human matrix metalloproteinase-2 and -9 to tissue inhibitor of metalloproteinase (TIMP)-1 and TIMP-2. *J. Biol. Chem.* 272:29975–29983.

Quigley, J. P., and D. A. Cheresh. 1996. Localization of matrix metalloproteinase MMP-2 to the surface of invasive cells by interaction with integrin alpha v beta 3. *Cell.* 85:683–693.

Petersen, N. O., and E. L. Elson. 1986. Measurements of diffusion and chemical kinetics by fluorescence photobleaching recovery and fluorescence correlation spectroscopy. *Methods Enzymol.* 130:454–484.

Strongin, A. Y., I. Collier, G. Bannikov, B. L. Marmer, G. A. Grant, and G. I. Goldberg. 1995. Mechanism of cell surface activation of 72-kDa type IV collagenase: isolation of the activated form of the membrane metalloprotease. *J. Biol. Chem.* 270:5331–5338.

Strongin, A. Y., B. L. Marmer, G. A. Grant, and G. I. Goldberg. 1993. Plasma membrane-dependent activation of the 72-kDa type IV collagenase is prevented by complex formation with TIMP-2. *J. Biol. Chem.* 268:14033–14039.

Trojanowska, M., E. C. LeRoy, B. Eckes, and T. Krieg. 1998. Pathogenesis of fibrosis: type 1 collagen and the skin. *J. Mol. Med.* 76:266–274.

Vu, T. H., and Z. Werb. 2000. Matrix metalloproteinases: effectors of development and normal physiology. *Genes Dev.* 14:2123–2133.

Werb, Z., and J. R. Chin. 1998. Extracellular matrix remodeling during morphogenesis. *Ann. NY Acad. Sci.* 857:110–118.

Wilhelm, S. M., I. E. Collier, A. Kronberger, A. Z. Eisen, B. L. Marmer, G. A. Grant, E. A. Bauer, and G. I. Goldberg. 1987. Human skin fibroblast stromelysin: structure, glycosylation, substrate specificity, and differential expression in normal and tumorigenic cells. *Proc. Natl. Acad. Sci. U.S.A.* 84:6725–6729.

Wilhelm, S. M., I. E. Collier, B. L. Marmer, A. Z. Eisen, G. A. Grant, and G. I. Goldberg. 1989. SV40 transformed human lung fibroblasts secrete a 92 kDa type IV collagenase which is identical to that secreted by normal human alveolar macrophages. *J. Biol. Chem.* 264:17213–17221.

Wolfram, S. 1999. The Mathematica Book. Wolfram Media/Cambridge University Press, New York.

Woodhouse, E. C., R. F. Chuaqui, and L. A. Liotta. 1997. General mechanisms of metastasis. *Cancer.* 80:1529–1537.

Yurchenko, P. D., D. E. Birk, and R. P. Mecham, editors. 1994. Extracellular Matrix Assembly and Structure. Academic Press, San Diego.